

Thermogravimetric Measurement of the Vapor Pressure of Iron from 1573 K to 1973 K

Frank T. Ferguson,^{‡,*} Joseph A. Nuth, III,[†] and Natasha M. Johnson^{†,§}

Code 691, NASA–Goddard Space Flight Center, Greenbelt, Maryland 20771, and Department of Chemistry, Catholic University of America, Washington, D.C. 20064

The vapor-pressure data of iron was measured using the combination of a Knudsen effusion cell and a high-temperature, thermogravimetric balance. Most of the available vapor-pressure data for iron have been taken below 1600 K. In contrast, the current data have been collected from 1573 to 1973 K, and these values should help fill a void in the data near the melting point of iron. Although the measured vapor pressures have a similar temperature dependence as literature values of iron vapor-pressure data, the current data is consistently lower than these previous values by roughly a factor of 2.

Introduction

An accurate knowledge of the vapor pressure of iron is crucial to a variety of fields including the vapor-phase nucleation and growth of ultrafine metal particles in aerosol reactors for use in catalysis or nanotechnology^{1,2} or in understanding the condensation sequence of metals in meteorites in the early solar nebula.³ Unfortunately, most of the available vapor-pressure data for iron has been taken under 1600 K, well below the melting point. In this paper, we report results for a series of iron vapor-pressure measurements taken from approximately 1573 K to 1973 K. The prevailing vapor pressures within this temperature range (roughly 0.1 Pa to 10 Pa) are well suited for study using a Knudsen effusion cell. We have constructed such a cell in our laboratory and measured the vapor pressure of iron by monitoring the mass loss from the effusion cell using a high-temperature, thermogravimetric (TG) balance.

Experimental Equipment

Vapor-pressure measurements were made using a Knudsen effusion cell and a CAHN TG 2171 TG balance. This balance can be operated to a maximum temperature of 1973 K and is able to accept sample sizes as large as 0.1 kg with microgram sensitivity. Sample cells were suspended from a thin, alumina rod attached to one arm of the TG balance. During operation, the cell was placed within a larger 99.8% alumina reactor tube of approximately 3.5×10^{-4} m³ volume. The sample cell temperature was measured using an alumina-sheathed, type-B thermocouple, which is positioned just under the bottom of the sample cell.

A picture of the Knudsen cell constructed for these experiments is shown in Figure 1. Cells were constructed from two, closed-end, 99.8% alumina tubes of differing diameters. The outside diameter of the smaller tube (9.53×10^{-3} m outside diameter, 6.35×10^{-3} m inside diameter) was chosen so that it was just slightly smaller than the inside diameter of the larger tube (9.53×10^{-3} m inside

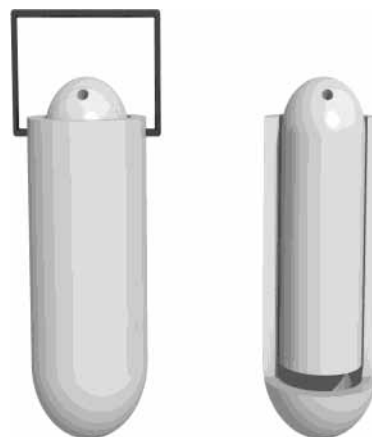


Figure 1. Alumina effusion cell constructed from closed-end tubes.

diameter, 1.27×10^{-2} m outside diameter). The length of the smaller tube was then cut such that the closed end of the tube rested just slightly above the lip of the larger tube as shown in Figure 1. At the top of the smaller tube, a small hole was drilled using a diamond-coated drill bit. This hole was drilled at a 45° angle relative to the centerline of the tube to avoid possible condensation on the hangdown assembly, resulting in an underestimate of the actual effusion rate. After the two alumina tubes were cut and the hole drilled in the inner tube, a sample of iron (99.97% purity) was placed within the cell. To avoid possible leaks of iron vapor between the tube walls, the gap between the two was sealed at the top using a high-temperature, zirconia adhesive (Resbond 904, Cotronics Corporation). A small length of molybdenum wire was formed in a loop and was used to attach the cell to the balance hangdown assembly. Although single sample cells can be used for several runs, once sealed they cannot be reopened and refilled with metal.

The balance is capable of operating with a slow, continuous flow of reactant or inert gases passing through the reactor volume or with the reactor tube and balance assembly under vacuum using an additional vacuum attachment. Iron vapor-pressure measurements were carried out under vacuum, and the reactor volume was pumped using

* To whom correspondence may be addressed. E-mail: frank.ferguson@gsfc.nasa.gov.

[†] NASA–Goddard Space Flight Center.

[‡] Catholic University of America.

[§] National Research Council Research Associate.

a mechanical and turbomolecular pump combination. During the vapor-pressure measurements and throughout the entire temperature range, the vacuum within the reactor volume was maintained under 0.01 Pa

Experimental Procedure

After the components of a cell were constructed, a sample of high-purity (99.97%) iron was placed within the tubes, high-temperature adhesive was applied to the seam between the two cell walls, and the cell was allowed to dry at room temperature overnight. After drying, the hole size was estimated using a caliper and a series of finely graduated drill bits. The largest drill size that would pass through the cell orifice was measured with a high-accuracy caliper. Hole sizes of 2.0 and 3.0 mm were used in the iron experiments, and we estimate an error in the hole size measurement for both orifices of ± 0.2 mm. The cell was then placed within the balance and the reactor volume evacuated. To ensure that no volatiles in the adhesive persisted (possibly causing an error in the mass loss rate), the cell was initially heated to 200 °C and held at that temperature for approximately an hour. It was then raised to 700 °C and held for several hours. At both temperatures, the mass was continuously monitored to verify that the cell lost no mass.

During an experimental run, the cell was heated to a maximum temperature and then held at various lower temperatures for fixed times, continuously recording the cell mass and temperature at the rate of one measurement per second. These isothermal periods could range from 30 to 45 min at the highest temperatures to as long as 4 h at the lowest temperatures where the loss rate was very low. In some Knudsen cell measurements where the mass loss is determined by weighing the cell at the beginning and end of a run, there is the possibility of mass-loss errors while the cell is being heated to temperature and cooled back down. Also, measurements in this case can be time consuming since only a single data point can be collected per run. Since mass measurements are continuously available with the current system, several measurements at different temperatures can be made in a single run.

Data Collection and Vapor-Pressure Calculation

During an experiment, changes in sample mass with temperature were recorded continuously at the rate of one per second. After the run, the data were processed in the following manner: Values for the temperatures and mass were averaged over 5-min intervals. These mass data were then used to calculate the rate of mass loss as a function of time by simply taking the differences in the rate of mass loss occurring over these 5-min intervals. Over regions where the temperature remained isothermal, the average mass loss as a function of time was calculated. The standard deviation of this mean mass-loss rate was taken as an estimate of the error in this value. At an absolute temperature, T , the rate of mass loss from the cell is given by the Hertz–Knudsen equation for effusion in a vacuum⁴

$$\frac{dm}{dt} = PS \left(\frac{M}{2\pi RT} \right)^{1/2} \quad (1)$$

where (dm/dt) is the rate of mass loss, P is the equilibrium vapor pressure, S is the cross sectional area of the effusion orifice, M is the molecular weight of the evaporating material, and R is the ideal gas constant. Therefore, P is calculated from the mean mass-loss rate for a given temperature isotherm.

Two corrections are applied to the vapor pressure calculated via eq 1. First, if the orifice in the Knudsen cell is not infinitely thin, there is a correction for back reflection of atoms through a short “pipe” rather than a knife-edged orifice. Clausing⁴ collected and tabulated data for the effusion of gases through an orifice of finite wall thickness, and Kennard⁵ presented empirical formulas to represent these correction factors. If the depth of the hole (wall thickness) is denoted by L and the radius of the hole is R , then for (L/R) between 0 and 1.5, the Kennard formula for the Clausing correction factor, K , is given by⁴

$$K = \frac{1}{1 + 0.5(L/R)} \quad (2)$$

For values of (L/R) greater than 1.5

$$K = \frac{1 + 0.4(L/R)}{1 + 0.95(L/R) + 0.15(L/R)^2} \quad (3)$$

The values of (L/R) for all of the experimental points within this work were less than 1.5, and eq 2 was used to compute the Clausing correction factor.

Second, the loss of the vapor through the hole must cause a disturbance to the equilibrium within the cell. A correction, σ , for this is given by⁴

$$\sigma = \frac{1}{1 + \frac{aK}{A\alpha}} \quad (4)$$

where K is the Clausing factor, a is the cross-sectional area of the orifice, A is the area of the evaporating material, and α is the evaporation accommodation coefficient. With these two corrections, the corrected equilibrium vapor pressure, $P_{\text{corrected}}$, is calculated via

$$P_{\text{corrected}} = \frac{P}{\sigma K} \quad (5)$$

Temperature Calibration

To verify the type-B thermocouple accuracy, we performed the following calibration. A small piece of iron was cut, and a small hole was drilled through the iron. A length of molybdenum wire was passed through the hole and attached to the balance hangdown assembly such that it was in the exact position where the cell is normally positioned. The furnace was then heated to just below the melting point of iron. At this point, the heating rate was greatly reduced (to a rate of 0.5 K/min) and the furnace temperature was slowly raised above the melting point of iron. As shown in Figure 2, in the vicinity of the melting point, there was an abrupt change in mass associated with the melting of the iron sample. In our measurements, this occurred at approximately 1810 K, very close to the accepted melting-point value for iron of 1811 K.⁶ On the basis of this simple test, we conclude that the thermocouple used for these experiments was functioning correctly and we assume that all errors associated with thermocouple measurements are equal to the expected measurement errors associated with type-B thermocouples over the temperature range, approximately ± 3 K.

Experimental Results

Mass-loss experiments were performed with two different effusion cells with holes of 2.0 and 3.0 mm, and the calculated vapor-pressure data from both sets of data is shown in Table 1. In addition, these new vapor-

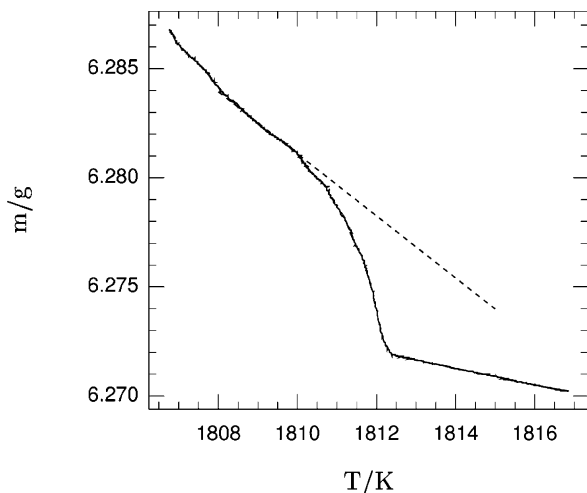


Figure 2. Verification of thermocouple accuracy using the melting point of iron.

Table 1. Experimental Data for Iron Vapor-Pressure Measurements

T/K	d/mm	P/Pa	wt loss/mg	t/s
1973	2	$16. \pm 4$	25.2	1200
1923	2	8 ± 2	18.2	1800
1873	2	3.7 ± 0.9	13.5	2700
1823	2	1.8 ± 0.4	6.5	2700
1773	2	0.8 ± 0.2	5.1	4500
1723	2	0.34 ± 0.09	2.1	4500
1673	2	0.16 ± 0.05	1.4	6300
1973	2	13 ± 3	29.6	1800
1948	2	9 ± 2	23.6	2100
1898	2	4.1 ± 0.9	16.4	3000
1848	2	2.0 ± 0.5	8.0	3000
1798	2	1.0 ± 0.2	4.0	3000
1873	2	4 ± 1	3.6	600
1973	2	9 ± 2	25.9	2100
1923	2	5 ± 1	13.7	2100
1873	2	2.5 ± 0.6	10.1	3000
1823	2	1.3 ± 0.3	5.3	3000
1773	2	0.6 ± 0.2	4.1	4800
1723	2	0.29 ± 0.07	1.9	4800
1673	2	0.20 ± 0.05	1.3	4800
1973	3	11 ± 1	10.6	300
1923	3	5.8 ± 0.8	16.9	900
1873	3	3.0 ± 0.4	8.8	900
1823	3	1.4 ± 0.2	7.1	1500
1773	3	0.66 ± 0.09	4.0	1800
1723	3	0.33 ± 0.04	2.0	1800
1673	3	0.16 ± 0.03	1.0	1800
1961	3	$9. \pm 1$	8.7	300
1936	3	6.6 ± 0.9	25.3	1200
1911	3	4.9 ± 0.7	19.0	1200
1886	3	3.6 ± 0.7	13.7	1200
1861	3	3 ± 1	9.9	1200
1836	3	1.7 ± 0.3	6.7	1200
1786	3	0.8 ± 0.2	3.2	1200
1748	3	0.3 ± 0.3	1.9	2100
1698	3	0.3 ± 0.2	1.9	1800
1886	3	3.7 ± 0.5	10.7	900
1861	3	2.6 ± 0.3	7.5	900
1836	3	1.8 ± 0.2	5.3	900
1811	3	1.2 ± 0.2	3.7	900
1786	3	0.9 ± 0.1	2.6	900
1748	3	0.47 ± 0.06	3.4	2100
1698	3	0.19 ± 0.03	1.4	2100
1623	3	0.05 ± 0.01	0.8	4500
1573	3	0.02 ± 0.01	0.3	4500

pressure results are plotted in Figure 3. The expected error in the temperature measurement is given by the error limits over the temperature range for a type-B thermocouple. In most cases, this error is comparable to the size of the symbol. For the vapor-pressure data, the two most

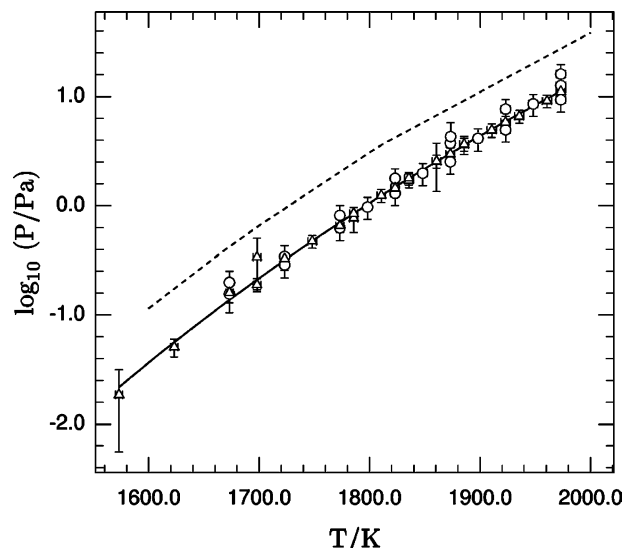


Figure 3. Measured iron vapor pressure for both effusion cell orifice diameters. Shown in the figure are data points for the: \circ , 2-mm hole size; and \triangle , 3-mm hole size. Also shown in the figure is the fit to the data (solid line) and a comparison with the iron vapor-pressure compilation by Desai⁷ 1986 (dashed line).

significant sources of error arise due to the measurement of the effusion hole diameter (estimated at ± 0.2 mm) and from the standard deviation of the calculated mean mass-loss rate. In most cases, the error in the hole diameter dominates and is responsible for most of the vertical error bars in Figure 3. In a few cases in which the noise in the mass measurement was larger than typical, the error in the mean mass-loss rate dominates and this increased noise level is responsible for the much larger error bars for several points from a single run with the 3-mm hole size.

In the equations used to calculate the iron vapor pressure, the accommodation coefficient is unknown. Often this term is assumed to be equal to 1, but Nesmeyanov warns that this is often not true.⁴ For example, values for the accommodation coefficient as low as 3×10^{-4} and 6×10^{-4} have been reported for cobalt and nickel, respectively.⁴ In contrast, Marshall et al. concluded that the values of the accommodation coefficient for copper and iron were near unity.⁷ With a Knudsen cell, Nesmeyanov suggests a method for estimating the value of this coefficient.⁴ First, two different experiments are run with different hole sizes. Then, an estimate of the accommodation coefficient is made by comparing the discrepancy between the two different vapor pressures calculated at a given temperature and adjusting the value of the accommodation coefficient until the discrepancy between the two measurements is minimized.

On first view, both of our sets of data with different hole sizes seemed to give identical results, implying that the accommodation coefficient was 1.0. To verify this, we recalculated the data with different values of the accommodation coefficient but found that a value of $\alpha = 1.0$ produced the least discrepancy between the two data sets.

A weighted, least-squares fit to the range of data yielded the following equation for the vapor pressure

$$\log_{10}(P/Pa) = (11.7 \pm 0.3) - \frac{21000 \pm 500}{TK} \quad (6)$$

Weighting factors for this fit were constructed from the inverse of the square of the error levels as given in Table

1, and this fit through the experimental data is also shown in Figure 3.

In 1986, Desai presented a review and compilation of available vapor-pressure data for iron.⁶ From these collected works, he calculated a weighted, average value for the enthalpy of sublimation of iron at 298.15 K. Using this best estimate for the enthalpy of sublimation and available heat capacity data for iron, he then estimated the vapor pressure of iron over a wide temperature range. The vapor-pressure values from his compilation were nearly identical to an earlier compilation by Hultgren et al.⁸ and approximately a factor of 2 lower than a much earlier compilation by Nesmeyanov.⁴ The results of this compilation over the experimental temperature range in this work are also shown in Figure 3. As shown in the figure, the two datasets have consistent slopes, indicating similar heats of vaporization, but the experimental data collected in this work are approximately a factor of 2 lower than the compilation by Desai. Also, the discrepancy between the two is well beyond the estimated error levels we have placed on the vapor-pressure data in this current work based on errors in the temperature measurement, mass-loss rate, and effusion hole size determination.

On the basis of our fit to the data, we estimate the enthalpy of vaporization to be $\Delta H = 403 \pm 8$ kJ/mol over the experimental temperature range. By application of the Third Law to the data combined with the thermodynamic data from Desai,⁶ we calculated the enthalpy of vaporization at 298.15 K for each of our experimental vapor-pressure points. By assumption of negligible error in the thermodynamic data, the error levels for the individual data points shown in Figure 3 and Table 1 correspond to an approximately ± 3 kJ/mol deviation in individual enthalpy calculations. An inverse square of these individual error levels was used to calculate a mean enthalpy of vaporization at 298.15 K of $\Delta H = 431.2 \pm 0.4$ kJ/mol, where the error level is based on the standard deviation of this mean value. The individual enthalpy values used to calculate this mean value were randomly scattered about this mean value and did not show any systematic variation with temperature. For comparison, Desai estimated this value to be 415 ± 1 kJ/mol.⁶

A comparison between the current experimental data and other published data over approximately the same temperature range is shown in Figure 4. Again, as in Figure 3, the estimated vapor pressure from the compilation by Desai⁶ is shown in the figure. As noted earlier, much of the available vapor-pressure data for iron has been taken below 1600 K. For clarity, many of these studies have not been included in Figure 4. For further information on these data, the reader is urged to consult the references available in the most recent compilation of iron properties by Desai⁶ or earlier compilations by Hultgren et al.⁸ and Nesmeyanov.⁴

In Figure 4, the available iron vapor-pressure data sets above approximately 1500 K has been plotted along with the current experimental data and the compilation by Desai.⁶ The vertical scale has been expanded in this figure to highlight differences between the different vapor-pressure experiments. Also, the single, vertical line in the plot denotes the melting point of iron.

If individual data points were available, they were plotted as symbols in Figure 4.^{9–17} In the case of four experimental studies, only fits to the experimental data were provided and line segments represent these data over the temperature region where the experiments were conducted.^{18–21} Only the data from Chegodaev et al.¹⁹ is

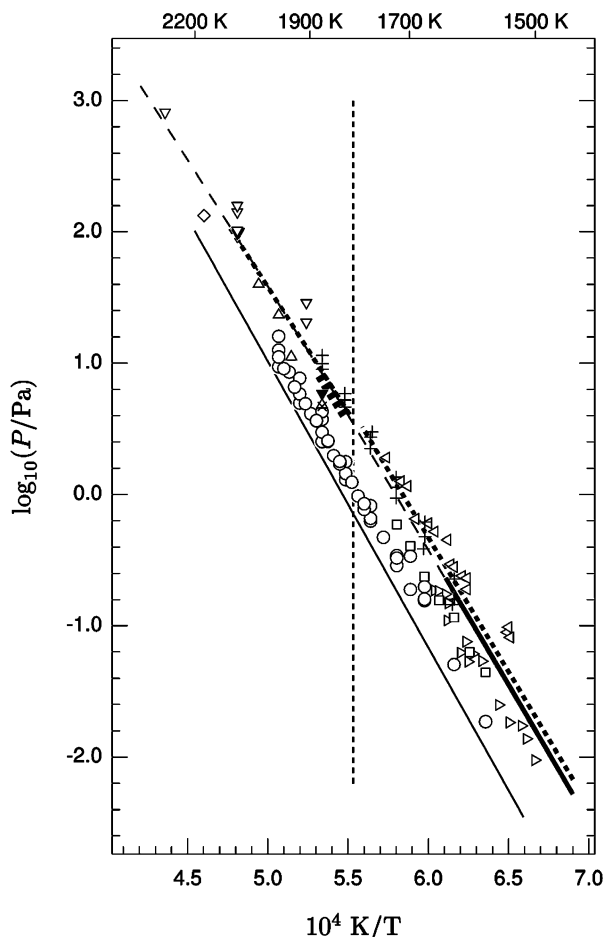


Figure 4. Comparison between the current experimental iron vapor-pressure data and available published data. Shown in the figure are experimental data from: \circ , the current experimental work; \blacktriangledown , Darken and Gurry,⁹ 1946; \diamond , Mikulinskii and Umova,¹⁰ triangle pointing right, Wessel,¹¹ 1951; triangle pointing left, Vintaikin,¹² 1957; \times , Turkdogan and Leake,¹³ 1960; \square , Smith and Shuttleworth,¹⁴ 1965; \triangle , Karasev et al.,¹⁵ 1971; ∇ , Yavoiskii et al.,¹⁶ 1971; and $+$, Lindscheid and Lange,¹⁷ 1975. Fits to experimentally measured data are shown for Zellars et al.,¹⁸ 1959 (bold dotted line); Chegodaev et al.,¹⁹ 1978 (solid line); Bodrov et al.,²⁰ 1982 (dotted line); and Zaitsev et al.,²¹ 1990 (bold solid line). The compilation of iron data by Desai 1986 (dashed line) is also shown in the figure.

consistently lower than the current experimental work. Data from the works of Karasev et al.,¹⁵ Turkdogan and Leake,¹³ Vintaikin,¹² and Smith and Shuttleworth¹⁴ are comparable to our results, while the remaining points are approximately a factor of 2 higher. Again, as noted earlier, this discrepancy is well beyond that attributable to estimated errors in the temperature measurement, mass-loss rate, or effusion hole size determination. It should be noted that, although the data collected in this work indicates a lower vapor pressure than suggested by many of these previous works, the current data is nearly parallel with these previous data, indicating a similar enthalpy of vaporization.

Summary

We have completed a study of iron vapor pressure using the combination of a Knudsen effusion cell and a high-temperature TG balance. Several runs were taken with two different effusion cells covering a temperature range from 1573 K to 1973 K, and both cells gave consistent results. Although the iron vapor-pressure data have a slope that

is consistent with compiled reviews of iron vapor pressure from previous works, the current data is lower than most of these previous measurements by a factor as large as 2.

Literature Cited

- (1) Girshick, S. L.; Chiu, C. P.; Muno, R.; Wu, C. Y.; Yang, L.; Singh, S. K.; McMurry, P. H. Thermal Plasma Synthesis of Ultrafine Iron Particles. *J. Aerosol Sci.* **1993**, *24*, 367–382.
- (2) Singh, Y.; Javier, J. R. N.; Ehrman, S. H.; Magnusson, M. H.; Deppert, K. Approaches to increasing yield in evaporation/condensation nanoparticle generation. *J. of Aerosol Sci.* **2002**, *33*, 1309–1325.
- (3) Meibom, A.; Desch, S. J.; Krot, A. N.; Cuzzi, J. N.; Petaev, M. I.; Wilson, L.; Keil, K. Large-Scale Thermal Events in the Solar Nebula: Evidence from Fe, Ni Metal Grains in Primitive Meteorites. *Science* **2000**, *288*, 839–841.
- (4) Nesmeyanov, A. N. *Vapor Pressure of the Elements*; Academic Press: New York, 1963.
- (5) Kennard, E. H. *Kinetic Theory of Gases*; McGraw-Hill Book Company: New York, 1938.
- (6) Desai, P. D. Thermodynamic Properties of Iron and Silicon. *J. Phys. Chem. Ref. Data* **1986**, *15* 967–983.
- (7) Marshall, A. L.; Dorn, R. W.; Norton, F. J. The Vapor Pressure of Copper and Iron. *J. Am. Chem. Soc.* **1937**, *59*, 1161–1166.
- (8) Hultgren, R.; Desai, P. D.; Hawkins, D. T.; Gleiser, M.; Kelley, K. K.; Wagman, D. D. *Selected Values of the Thermodynamic Properties of the Elements*; American Society for Metals: Metals Park, Ohio, 1973.
- (9) Darken, L. S.; Gurry, R. W. The System Iron–Oxygen. II. Equilibrium and Thermodynamics of Liquid Oxide and Other Phases. *J. Am. Chem. Soc.* **1946**, *68*, 798–816.
- (10) Mikulinskii, A. S.; Umova, M. A. Determination of the Vapour Tension of Aluminium over its Ferroalloys by a Kinetic Method. *Theory and Practice of Electrothermal Ore Treatment*; Sverdlovsk: Moscow, 1948.
- (11) Wessel, G.; Measurement of the Vapor Pressure and Condensation Coefficient for Iron, Cadmium and Silver. *Z. Phys.* **1951**, *130*, 539–548.
- (12) Vintaikin, E. Z. Determination of Iron Vapor Pressure over Austenite. *Dokl. Akad. Nauk SSSR* **1957**, *117*, 632–634.
- (13) Turkdogan, E. T.; Leake, L. E. Vapor Pressure of Iron at 1600 °C. *Trans. Metal. Soc. AIME* **1960**, *218*, 1136–1137.
- (14) Smith, R.; Shuttleworth, R. The Vapor Pressure of Solid Iron. *Trans. Metal. Soc. AIME* **1965**, *233*, 806–808.
- (15) Karasev, Y. A.; Tsemekhman, L. S.; Vaisburd, S. E. Vapour Pressure of Iron, Cobalt, and Copper above the Melting Point. *Russ. J. Phys. Chem.* **1971**, *45*, 1172–1173.
- (16) Yavoiskii, V. I.; Svyazhin, A. G.; Vishkarev, A. F.; Nguyen, K. B.; Romanovich, D. A.; Chursin, G. M. Iron Vapor Pressure over Liquid Iron and Iron–Carbon Melts. *Izv. Akad. Nauk SSSR Metall.* **1971**, *3*, 33–40.
- (17) Lindscheid, H.; Lange, K. W. Measurements of the Vapor Pressures of Manganese, Iron and Palladium with a Knudsen-Torsion Apparatus. *Z. Metallkd.* **1975**, *66*, 546–547.
- (18) Zellars, G. R.; Payne, S. L.; Morris, J. P.; Kipp, R. L. The Activities of Iron and Nickel in Liquid Fe–Ni Alloys. *Trans. Metal. Soc. AIME* **1959**, *215*, 181–185.
- (19) Chegodaev, A. I.; Dubinin, E. L.; Tomofeev, A. I.; Vatolin, N. A.; Kapitanov, V. I. Vapor Pressure of Molten Metals at High Temperatures. *Zh. Fiz. Khim.* **1978**, *52*, 2124.
- (20) Bodrov, N. V.; Nikolayev, G. I.; Nemets, A. M. Vapour Pressure of Iron. *Russ. Metall.* **1982**, *2*, 35–39.
- (21) Zaitsev, A. I.; Zemchenko, M. A.; Mogutnov, B. M. Vapor Pressure of Iron. *Zh. Fiz. Khim.* **1990**, *64*, 3377–3378.

Received for review August 5, 2003. Accepted February 23, 2004.

JE034152W